

Non-hydrostatic modelling with the GEM model

**Jean Côté, Claude Girard, André Plante, Ron McTaggart-Cowan
Jason Milbrandt, Abdessamad Qaddouri**

*Recherche en prévision numérique and Canadian Meteorological Centre
Environment Canada, Dorval, CANADA
jean.cote@ec.gc.ca*

Abstract

A brief review of non-hydrostatic modelling in Canada is presented in the introduction. We present next a reformulation of the vertical structure to accommodate the Charney-Phillips vertical staggering along with a modification of the vertical coordinate since this is the current configuration of the non-hydrostatic version of the GEM model. This model in a limited-area configuration was used operationally for high-resolution (1-km grid spacing) non-hydrostatic forecasting for the Vancouver Olympics. The knowledge acquired with the Olympics LAM will be transferred to the LAM windows currently run at 2.5 km and used quasi-operationally over Canada. The forecast issued from these models will eventually acquire the operational status.

1. Introduction

Non-hydrostatic modelling in Canada began with Tanguay *et al.* (1990). Building on a previous limited-area model of Robert that was already semi-implicit semi-Lagrangian (SISL), the vertical momentum equation was added to the set of primitive equations and the hydrostatic approximation was relaxed. The model used height above ground as its vertical coordinate and the SISL algorithm was shown to apply without too much overhead to this expanded set of equations where the acoustic modes were not filtered but distorted. The rationale was that by removing a constraint on the equation set one would be closer to the exact equations describing the real atmosphere and better physics parameterizations would follow for higher resolution modelling.

This model had simplified physics, no topography and served only as a proof of concept. It was further developed with full physics and topography and became known as the “Mesoscale Compressible Community” (MC2) model. It was later optimized (Benoit *et al.*, 1997, Girard *et al.*, 2005) and served the research community in Canada and abroad. It was used, for example, to provide numerical guidance for the first Mesoscale Alpine Programme (MAP) (Benoit *et al.*, 2002).

At the suggestion of Robert, Laprise (1992) examined “hydrostatic pressure” as a basis for a pressure-based vertical coordinate for non-hydrostatic modelling. The “Global Environment Multiscale” (GEM) model was in development at the time and this fitted perfectly with the objectives of the model to be hydrostatic for large-scale forecasts and non-hydrostatic for fine-scale forecasts. Furthermore, one could use most of the physical parameterizations developed for pressure-based hydrostatic forecasting. Hydrostatic pressure reverts to ordinary pressure in hydrostatic mode and this makes it easier to switch between modes. It appears that, independently, a similar thinking led to the development of ARPEGE/Aladin NWP system (Bubnová *et al.*, 1995).

The GEM model became operational in Canada in 1997 with the hydrostatic approximation (Côté *et al.*, 1998a, b). It was first used in hydrostatic mode with a global variable-resolution grid at 35 km spacing for (continental scale) regional forecasting. Later that year, daily experimental (quasi-operational status) “High-resolution Meteorological APplication” (HiMAP) runs were implemented at 15 km with smaller grids centred on the eastern and western parts of Canada respectively. In 1998, the

resolution of the regional configuration was increased to 24 km and the model also became operational for data assimilation and global forecasting.

The validation of the GEM model in its non-hydrostatic configuration continued until 2001 (Yeh *et al.*, 2002). In that year the GEM model was used for a case study (Pine Lake Tornado) at 4 km (Erfani *et al.*, 2003) and to provide numerical guidance at 2.5 km grid spacing for the “Effects of Lake Breezes On Weather” (ELBOW) 2001 field experiment which was conducted in south-western Ontario during June to August of 2001 (King *et al.*, 2002). The use of the non-hydrostatic GEM model at 2.5 km was considered to be a success.

Up to that point the GEM model existed either in global uniform resolution or in global variable resolution modes. Mesoscale modellers were lobbying for a limited-area version, their main reason was that they only needed high-resolution over a small area (and short time) and did not want to be burdened with the cost of running a global model. A limited-area version (GEM-LAM) was therefore officially released on 7 February 2003. Some elements of the nesting strategy were borrowed from the experience gained with MC2 such as growing orography and hollow cube nesting.

A careful comparison of the variable resolution with the nested approach was performed (Gravel *et al.*, 2004, Gramann *et al.*, 2004, Erfani *et al.*, 2005). For example, using IOP-2B of MAP as a test case, the two approaches were found equivalent meteorologically, the GEM-LAM model being more efficient CPU-wise. A decision was then made to go with the limited-area approach for the high-resolution non-hydrostatic forecasting. Since 2005 there has been a staged implementation of LAM windows at 2.5 km resolution covering first southern British Columbia and Alberta (West), then Ontario and Quebec (East). Later on, Maritime and Arctic windows were added. They replaced the HiMAP forecasts in October 2005 and have inherited the quasi-operational status. For this model the physical parameterizations are also adapted to the resolution: the convection scheme is deactivated and a more detailed cloud microphysics scheme is used (Milbrandt and Yau, 2005).

The non-hydrostatic GEM-LAM also provided numerical guidance for several recent field experiments:

- 10 and 2.5 km windows for the Lunenburg Bay (NS) 2007 Demonstration Project. The goal was to develop a coupled atmosphere/ocean/biology/chemistry ecosystem model. The 2.5 km window was later expanded to become the quasi-operational Maritimes window.
- 15 and 2.5 km windows over the Alps for D-PHASE Operational Period from 1 June to 30 November 2007 (Rotach *et al.*, 2009a, b, McTaggart-Cowan *et al.*, 2010a, b).
- 1 km window embedded in an expanded West 2.5 km grid for the UNSTABLE 2008 project (Taylor *et al.*, 2010).
- Special operational forecast cascade to 1 km for the Vancouver Olympic and Paralympic Games (Joe *et al.*, 2010, Mailhot *et al.*, 2010). The Olympics’ set-up was relocalized over Ontario for G8/G20. A higher resolution urban scale model provided dispersion modelling.

2. New vertical structure

The original dynamical core has been recently reformulated and recoded in terms of a new vertical coordinate and staggered discretization on the Charney-Phillips grid.

For non-hydrostatic equations, pressure-type coordinates are replaced by coordinates of the hydrostatic-pressure type, $\pi = A(\eta) + B(\eta)\pi_s$ (Laprise, 1992), with π defined by the usual hydrostatic relation $\partial\pi/\partial z = -g\rho$. This coordinate corresponds to the original non-hydrostatic version of the GEM model (Yeh *et al.*, 2002). Introducing of $\phi = gz$ and μ , the non-hydrostatic index.

$$\mu = \frac{\partial p}{\partial \pi} - 1,$$

$$\frac{\partial \phi}{\partial \pi} = -\frac{RT}{p}.$$

The new vertical coordinate of the GEM model will be characterized by the label ζ . Numerically, it is given by $\zeta = \zeta_s + \ln \eta$ with $\zeta_s = \ln p_{ref}$ and $p_{ref} = 10^5$ Pa, a reference pressure. The following transformation rules apply:

$$\nabla_{\zeta} = \nabla_{\eta},$$

$$\frac{\partial}{\partial \zeta} = \eta \frac{\partial}{\partial \eta}.$$

The important difference comes from the specification of $\ln \pi$.

$$\ln \pi = A(\zeta) + B(\zeta)s,$$

where $s = \ln(\pi_s / p_{ref}) = \ln \pi_s - \zeta_s$ and with A and B given by

$$A = \zeta,$$

$$B = \left(\frac{\zeta - \zeta_T}{\zeta_s - \zeta_T} \right)^r,$$

where $\zeta_T = \ln \pi_T$, and the exponent r represents a coordinate rectification factor. To express the equations in terms of the basic model variables, a final transformation is required. $\ln(p)$ is replaced by $\ln \pi + \ln(p/\pi) = \zeta + Bs + q$, having defined the non-hydrostatic log-pressure deviation as $q = \ln(p/\pi)$, and replacing ϕ by $\phi' = \phi - \phi_*$ with $\phi_* = -RT_*(\zeta - \zeta_s)$ where T_* is a constant (we use $T_* = 240$ K). With the vertical discretization on the Charney-Phillips grid this gives:

$$\frac{d\mathbf{V}_h}{dt} + f\mathbf{k} \times \mathbf{V}_h + RT_* \bar{\zeta} \nabla_{\zeta} (Bs + q) + (1 + \bar{\mu}^{\zeta}) \nabla_{\zeta} \phi' = \mathbf{F}_h$$

$$\frac{dw}{dt} - g\mu = F_w$$

$$\frac{d}{dt} \left[\ln \left(\frac{T}{T_*} \right) - \kappa (Bs + \bar{q}^{\zeta}) \right] - \kappa \dot{\zeta} = \frac{Q}{c_p T}$$

$$\frac{d}{dt} [Bs + \ln(1 + \delta_{\zeta} Bs)] + \nabla_{\zeta} \cdot \mathbf{V}_h + \delta_{\zeta} \dot{\zeta} + \bar{\zeta}^{\zeta} = 0$$

$$\frac{d\bar{\phi}'^{\zeta}}{dt} - RT_* \dot{\zeta} - gw = 0$$

$$1 + \mu - e^{\bar{q}^\zeta} \left[\frac{\delta_\zeta q}{\delta_\zeta (\zeta + Bs)} + 1 \right] = 0$$

$$\frac{T}{T_*} + e^{\bar{q}^\zeta} \left[\frac{\delta_\zeta (\phi' / RT_* + Bs)}{\delta_\zeta (\zeta + Bs)} - 1 \right] = 0$$

where \mathbf{F}_h , F_w , Q are the source terms. The derivatives are replaced by simple finite differences represented by the operator δ_ζ and averaging operators represented by overbars are introduced where required. From the notation, it may be gathered that \mathbf{V}_h, q, ϕ' are defined on the same *momentum* or *full* levels. They are staggered with respect to $T, w, \mu, \dot{\zeta}$ that are placed on the same *thermodynamic* or *half* levels. Taking into account the boundary conditions, $\dot{\zeta} = 0$, it is natural to have half levels coincide with the top and bottom. This describes the essence of the vertical grid shown in Fig. 1.

Momentum levels					Thermodynamics levels
	—	ϕ_T, q_T	—	$\dot{\zeta}_T$	—
				T, w, μ
1	--	\mathbf{V}_h, ϕ, q	--	-----	--
	—	—————	—	$T, w, \mu, \dot{\zeta}$	—
2	--	\mathbf{V}_h, ϕ, q	--	-----	--
	—	—————	—	$T, w, \mu, \dot{\zeta}$	—
...	--	\mathbf{V}_h, ϕ, q	--	-----	--
	—	—————	—	$T, w, \mu, \dot{\zeta}$	—
N-1	--	\mathbf{V}_h, ϕ, q	--	-----	--
	—	—————	—	$T, w, \mu, \dot{\zeta}$	—
N	--	\mathbf{V}_h, ϕ, q	--	-----	--
				T, w, μ
	—	s, ϕ_S, q_S	—	$\dot{\zeta}_T$	—

Fig. 1. Charney-Phillips grid with N full levels.

The placement of horizontal momentum, thermodynamic, continuity and hydrostatic equations as well as horizontal wind, temperature, geopotential and vertical motion $\dot{\zeta}$ is the traditional one for hydrostatic models discretized on a Charney-Phillips grid, such as the original Canadian spectral model with finite differences in the vertical (Daley *et al.*, 1976). The placement of w on half levels is natural for non-hydrostatic models in height coordinates, for example the MC2 model. With this choice, the placement of the remaining equations and variables is straightforward. There are small irregularities near the boundaries in the placement of the variables; here we show T, w, μ slightly displaced for centred differencing. Further details are given in the paper by Girard *et al.* (2010)

3. Model for the Vancouver Olympic and Paralympic Games

The experimental deterministic system used for the Vancouver games is based on a high-resolution NWP model with improved geophysical fields, cloud microphysics and radiation schemes, and with new diagnostic model output. This mesoscale prediction system consists of three one-way-nested GEM-LAM grids (at 15-, 2.5-, and 1-km grid spacing; see Fig. 2) with the 1-km grid integrated for 19 h, twice a day, from the 0000 and 1200 UTC regional 15-km GEM operational runs (Mailhot et al. 2006). Note that data assimilation is only used in the regional 15-km GEM runs. (Currently, no special mesoscale data assimilation system is available for the high-resolution GEM-LAM grids, though research efforts towards this are underway.)

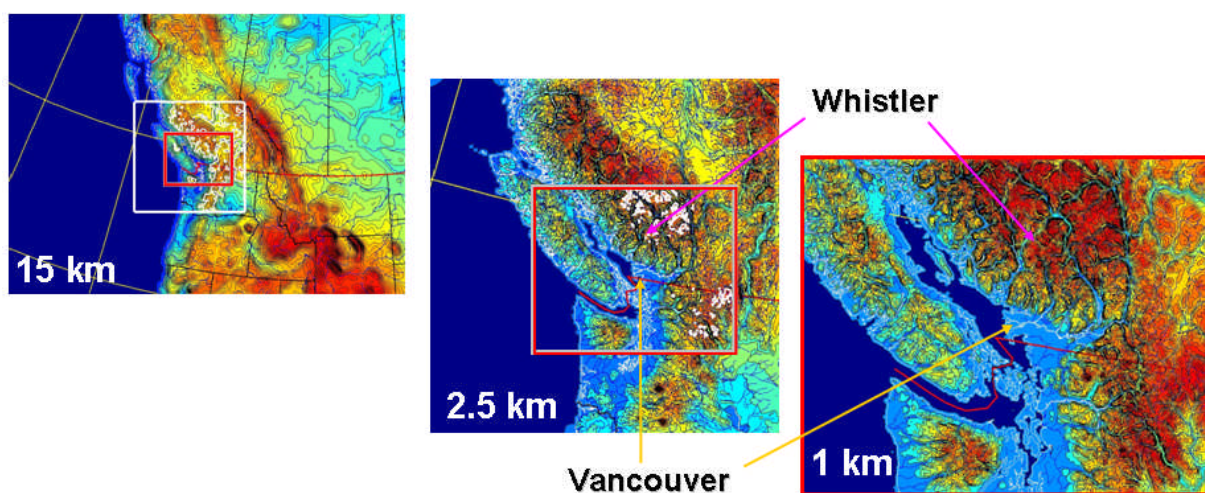


Fig 2. The domains of the high-resolution forecast prototype for the Olympics consisting of a cascade of three one-way nested grids with 15-km, 2.5-km, and 1-km horizontal grid-spacing covering the Vancouver and Whistler areas.

The configuration of the high-resolution modelling prototype is schematized in Fig. 3. The cascade of integrations goes the following way: 1) a GEM-LAM 15-km run is initialized from the 0-h forecast of the Regional GEM 15-km run started at 0000 UTC (boundary conditions for the GEM-LAM integration are also provided by the regional run) and integrated for 39 h until 1500 UTC the following day; 2) a GEM-LAM 2.5-km run is initialized at 0600 UTC from the 6-h forecast (allowing for the model spinup period) of the GEM-LAM 15-km run started at 0000 UTC (which also provides the boundary conditions) and integrated for 33 h until 1500 UTC the next day; 3) the GEM-LAM 1-km run is then initialized at 1100 UTC from the 5-h forecast of the 2.5-km run (which also provides the boundary conditions) and integrated for 19 h until 0600 UTC the next day. The same procedure is repeated for the regional 15-km GEM run starting at 1200 UTC to provide the Olympics cascade (15, 2.5, and 1 km) forecasts valid for the afternoon and evening (from 2000 to 1500 UTC; i.e., from 1200 to 0700 LT).

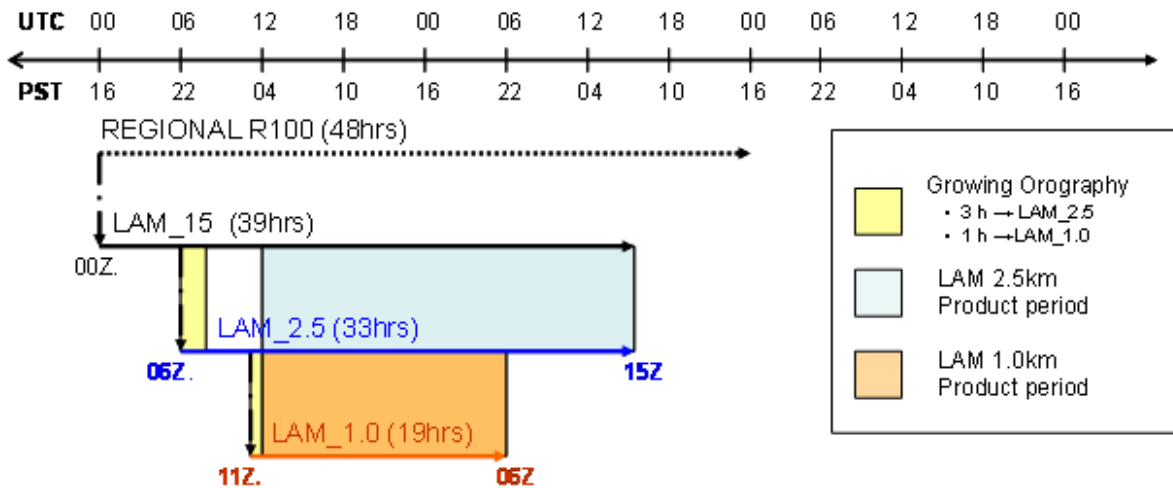


Fig 3. The daytime configuration (i.e. from 0000 UTC) of the high-resolution modelling prototype for the Vancouver 2010 Winter Olympics.

The 15- and 2.5-km grids of the Olympics system are essentially clones of the GEM-LAM system currently run quasi-operationally at CMC (Erfani et al. 2005), with the main differences being that they are integrated over a smaller domain and for a shorter period, and that they contain several improvements to the physics package, as follows:

- Geophysical fields: Improved orography, land–sea mask, and surface roughness length fields have been generated from a recent geophysical database at high resolution (90 m) using newly developed geophysical processor software.
- Cloud microphysics scheme: The prototype uses the double-moment version of the Milbrandt-Yau microphysics scheme (Milbrandt and Yau 2005) where two moments of the particle size distribution, proportional to the mass mixing ratio and total number concentration, respectively, of each of the six hydrometeor categories are independently predicted. The double-moment approach leads to more accurate calculations of the microphysical growth/decay rates (source/sink terms) and sedimentation (i.e., precipitation) rates compared to single-moment schemes Milbrandt and McTaggart-Cowan (2010), which predict only one moment (generally the mixing ratio), and are more commonly used due to of computational restraints. It also permits better identification of particle types, for example, the distinction between drizzle and rain, because the size distribution spectra can evolve more freely. Several other improvements to the microphysics parameterization have been made. This includes a diagnostic bulk snow density and a new precipitation rate (volume flux) of the total unmelted “snow” (based on the combined precipitation rates of the ice, snow, and graupel categories), which allows for the prediction of an instantaneous solid-to-liquid ratio for solid precipitation (Milbrandt et al. 2009).
- Radiation and cloud–radiation interactions: The radiative transfer scheme of Li and Barker (2005) has been included in the Olympic prototype, correcting the cold bias during winter conditions, seen previously, and providing more realistic temperature forecasts under such situations. Other components of the radiation package have also been improved, such as cloud-radiation interactions (cloud optical properties, liquid/solid partition, etc.).

Furthermore, emphasis was placed on developing several new diagnostic outputs from the high-resolution models, such as wind gusts, visibility, precipitation types, and snow-to-liquid ratio, all presented with a customized output package, as follows:

- Wind gusts and 10-m wind variances: near-surface wind gusts associated with surface layer turbulence and large eddies in the boundary layer are diagnosed from the turbulent variables in the model. Wind gusts [the wind gust estimate together with lower and upper bounds, based on the method of Brasseur (2001)] and standard deviations of 10-m wind speed and direction are available as 2D output fields.
- Visibility: The visibilities through fog (cloud water), rain, and snow, and “total” visibility (resulting from the combined effects of the reduction of visibility from all three) are available as 3D diagnostic output variables. The computations are based on empirical relations to the cloud water content and the droplet number concentration, and the precipitation rates of drizzle/rain and snow, respectively.
- Snow-to-liquid ratio of precipitating snow: As mentioned above, the snow-to-liquid ratio of falling snow is obtained as a new diagnostic output. This ratio can vary between values of around 2.5 (for very dense snow, either heavily rimed or partially melted) to values of over 30 (for very low-density snow, such as large aggregates).
- Various diagnostic levels: Several 2D fields have been added, such as the heights above ground of cloud base, freezing levels (either as the first 0°C isotherm from the ground or from above), and snow level (lowest level with a nonzero falling snow rate).
- Customized output package: Based on the feedback from the Olympics Forecast Team after the practicum periods of winters 2008 and 2009, a list of useful products was finalized, together with specifications related to the display format that could be easily used by the forecasters at the different Olympic venues. The comprehensive list of model outputs includes 2D maps, time series (meteograms) at a number of surface stations, cross sections along specific lines, and vertical soundings at standard and additional Olympic locations.

4. Verification for Vancouver Olympics LAM

Verification of the 2.5-km and 1-km LAM grids used for the Vancouver Olympics was performed in real-time, in hindcast, and continuing formal verification and evaluation is currently underway. A special Olympic Autostation Network (OAN) consisting of approximately 40 observation sites, for both standard and special surface observations, was deployed prior to the 2010 Olympics, concentrated in the small region in the vicinity of the venues. Meteorological variables from both the instruments and models were available in real time to researchers and forecasters (Fig. 4). This provided an excellent opportunity to evaluate the models in real time. It also allowed forecasters to determine whether or not they should have confidence in the model forecast during a given weather event even based on the skill of the model, compared to the in situ measurements, in the recent past.

After the games were complete, a formal verification of the modelling system began. The near-surface winds and temperatures from the model were scored against observations for various time periods.

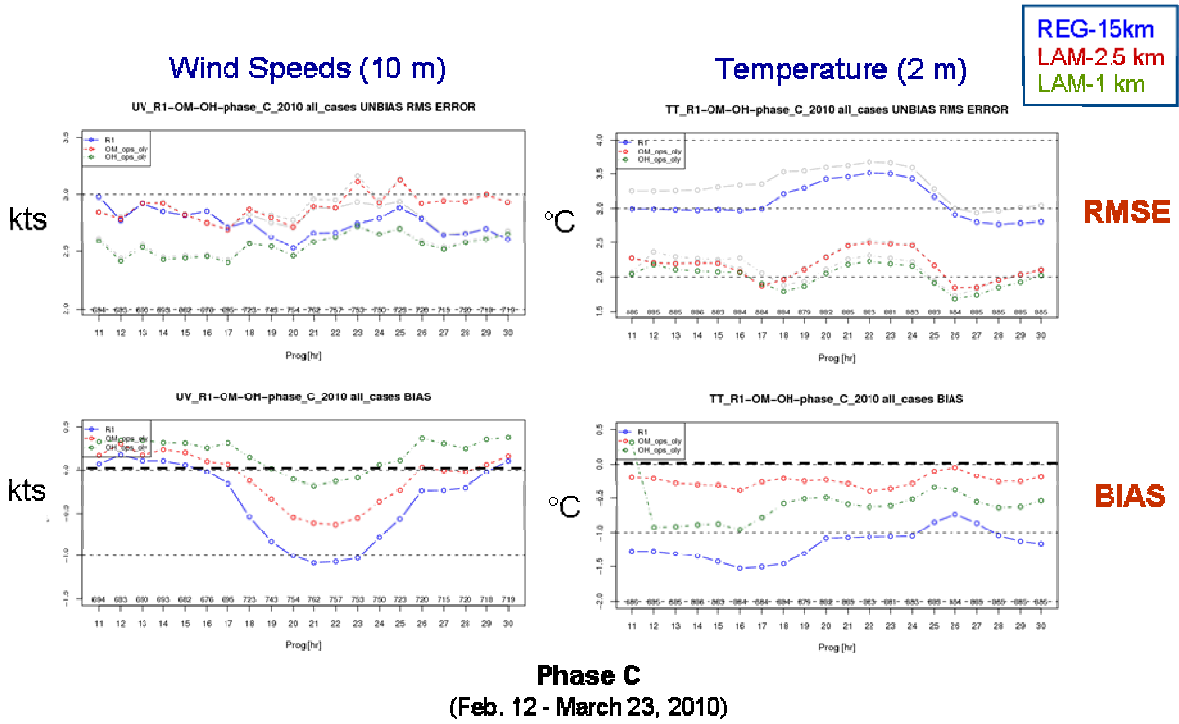


Fig. 4 Evaluation – Near-surface winds and temperature

The bias and the root-mean-square error were reduced for both the winds and temperature for the high-resolution models (Fig. 5). Continuing formal verification for other forecast variables in the

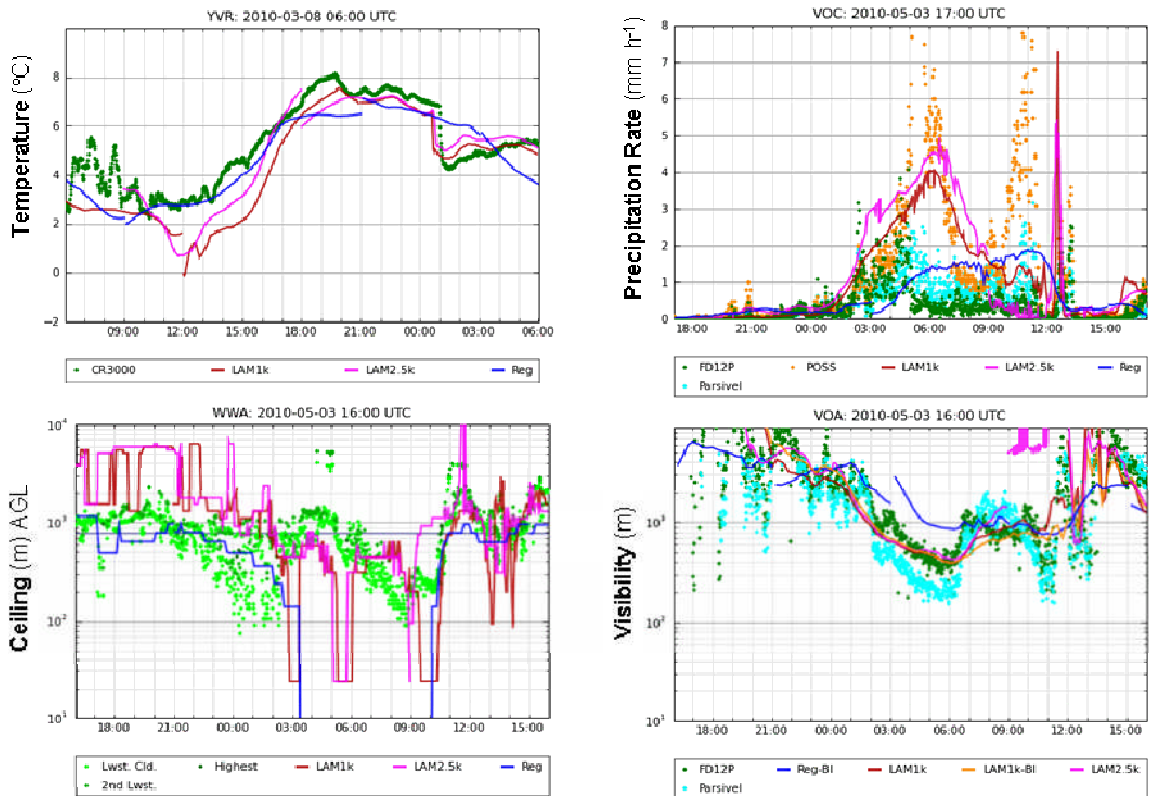


Fig. 5 Real-time verification examples (from SNOW-V10 site).

Olympic LAM system is ongoing. Once the entire final Olympic LAM configuration will have been validated, it will be ported to the LAM 2.5.

5. Conclusions

The LAMs at 2.5 km are now part of the day to day forecast guidance tools available for the Storm Prediction Centers in Canada. Furthermore, it has been a great learning experience for the Canadian Meteorological Center and the Meteorological Service of Canada for forecasting at this scale. The product is of sufficient maturity to become fully operational. It now remains to determine the final domains over which the LAMs will be run and how many times a day.

Acknowledgements. The authors would like to acknowledge the contributions to this presentation of Amin Erfani, André Giguère, Dov Bensimon, Richard Moffat and all those that were involved in the Vancouver Olympics project.

6. References

- Benoit, R., M. Desgagné, P. Pellerin, S. Pellerin, Y. Chartier, S. Desjardins, 1997: The Canadian MC2: A Semi-Lagrangian, Semi-Implicit Wideband Atmospheric Model Suited for Finescale Process Studies and Simulation, *Mon. Wea. Rev.*, **125**, 2382-2415.
- _____, C. Schär, P. Binder, S. Chamberland, H. C. Davies, M. Desgagné, C. Girard, C. Keil, N. Kouwen, D. Lüthi, D. Maric, E. Müller, P. Pellerin, J. Schmidli, F. Schubiger, C. Schwierz, M. Sprenger, A. Walser, S. Willemse, W. Yu, E. Zala, 2002: The Real-Time Ultrafinescale Forecast Support during the Special Observing Period of the MAP, *Bull. Amer. Meteor.*, **83**, 85-109.
- Bubnová, R., G. Hello, P. Bénard, J.-F. Geleyn, 1995: Integration of the Fully Elastic Equations Cast in the Hydrostatic Pressure Terrain-Following Coordinate in the Framework of the ARPEGE/Aladin NWP System, *Mon. Wea. Rev.*, **123**, 515-535.
- Côté, J., S. Gravel, A. Méthot, A. Patoine, M. Roch, A. Staniforth, 1998a: The Operational CMC–MRB Global Environmental Multiscale (GEM) Model. Part I: Design Considerations and Formulation, *Mon. Wea. Rev.*, **126**, 1373-1395.
- Côté, J., J.-G. Desmarais, S. Gravel, A. Méthot, A. Patoine, M. Roch, A. Staniforth, 1998b: The Operational CMC–MRB Global Environmental Multiscale (GEM) Model. Part II: Results, *Mon. Wea. Rev.*, **126**, 1397-1418.
- Daley, R., C. Girard, J. Henderson and I. Simmonds, 1976: Short-term forecasting with a multi-level spectral primitive equation model. Part I – Model Formulation. *Atmosphere*, **14**, 98-116.
- Erfani, A., A. Méthot, R. Goodson, S. Bélair, K.-S. Yeh, J. Côté and R. Moffet (2003): Synoptic and mesoscale study of a severe convective outbreak with the non-hydrostatic Global Environmental Multiscale (GEM) model, *Meteorol. Atmos. Phys.* **82**, 31-53.
- Erfani, A., J. Mailhot, S. Gravel, M. Desgagné, P. King, D. Sills, N. McLennan and D. Jacob, 2005: The high resolution limited area version of the Global Environmental Multiscale model and its potential operational applications. Preprints, *11th Conference on Mesoscale Processes*, Albuquerque, NM, Amer. Meteorol. Soc., CD-ROM Paper 1M.4
- Girard, C., R. Benoît, and M. Desgagné, 2005: Finescale topography and the MC2 Dynamics kernel. *Mon. Wea. Rev.*, **133**, 1463-1477.

- _____, A. Plante, J. Côté, A. Qaddouri, S. Gravel, M. Desgagné, L. Spacek, V. Lee, 2010: Staggered Vertical Discretization of the Canadian Nonhydrostatic Global Environmental Multiscale (GEM) Model using a coordinate of the log-hydrostatic-pressure type. To be submitted.
- Gramann, U., A. Erfani, J. Mailhot, S. Gravel, M. Roch, and L. Lefaiivre, 2004: Latest developments of the very high resolution Canadian Global Environmental Multiscale (GEM) model limited area version (GEM-LAM) over mountainous terrain. *11th Conference on Mountain Meteorology and the Annual Mesoscale Alpine Program (MAP)*, Bartlett, NH.
- Gravel, S., A. Erfani and U. Gramann, 2004: Latest developments of the very high resolution Canadian Global Environmental Multiscale (GEM) model limited area version (GEM-LAM) over mountainous terrain. *11th Conference on Mountain Meteorology and the Annual Mesoscale Alpine Program (MAP)*, Bartlett, NH.
- Joe, P., C. Doyle, A. Wallace, S. G. Cober, B. Scott, G. A. Isaac, T. Smith, J. Mailhot, B. Snyder, S. Bélair, Q. Jansen, B. Denis, 2010: Weather Services, Science Advances, and the Vancouver 2010 Olympic and Paralympic Winter Games, *Bull. Amer. Meteor.*, **91**, 31-36.
- King, P., B. Murphy, A. Erfani and D. Sills, 2002: The Use of the GEM forecast model at very high resolution during ELBOW 2001. *Preprints, 21st Severe Local Storms Conference*, San Antonio, TX, Amer. Meteorol. Soc., J125-J128
- Laprise, R., 1992: The Euler Equations of Motion with Hydrostatic Pressure as an Independent Variable, *Mon. Wea. Rev.*, **120**, 197-207.
- McTaggart-Cowan, R., T. J. Galarneau Jr., L. F. Bosart, J. A. Milbrandt, 2010: Development and Tropical Transition of an Alpine Lee Cyclone. Part I: Case Analysis and Evaluation of Numerical Guidance, *Mon. Wea. Rev.*, **138**, 2281-2307.
- McTaggart-Cowan, R., T. J. Galarneau Jr., L. F. Bosart, J. A. Milbrandt, 2010: Development and Tropical Transition of an Alpine Lee Cyclone. Part II: Orographic Influence on the Development Pathway, *Mon. Wea. Rev.*, **138**, 2308-2326.
- Mailhot, J., S. Bélair, M. Charron, C. Doyle, P. Joe, M. Abrahamowicz, N. B. Bernier, B. Denis, A. Erfani, R. Frenette, A. Giguère, G. A. Isaac, N. McLennan, R. McTaggart-Cowan, J. Milbrandt, L. Tong, 2010: Environment Canada's Experimental Numerical Weather Prediction Systems for the Vancouver 2010 Winter Olympic and Paralympic Games, *Bull. Amer. Meteor.*, **91**, 1073-1085.
- Milbrandt, J. A., R. McTaggart-Cowan, 2010: Sedimentation-Induced Errors in Bulk Microphysics Schemes, to appear in *Journal of the Atmospheric Sciences*.
- Milbrandt, J. A., M. K. Yau 2005: A Multimoment Bulk Microphysics Parameterization. Part II: A Proposed Three-Moment Closure and Scheme Description, *J. Atmos. Sci.*, **62**, 3065-3081.
- Rotach, M. W., P. Ambrosetti, C. Appenzeller, M. Arpagaus, L. Fontannaz, F. Fundel, U. Germann, A. Hering, M. A. Liniger, M. Stoll, A. Walser, F. Ament, H.-S. Bauer, A. Behrendt, V. Wulfmeyer, F. Bouttier, Y. Seity, A. Buzzi, S. Davolio, M. Corazza, M. Denhard, M. Dorninger, T. Gorgas, J. Frick, C. Hegg, M. Zappa, C. Keil, H. Volkert, C. Marsigli, A. Montaini, R. McTaggart-Cowan, K. Mylne, R. Ranzi, E. Richard, A. Rossa, D. Santos-Muñoz, C. Schär, M. Staudinger, Y. Wang, J. Werhahn, 2009: MAP D-PHASE: Real-Time

- Demonstration of Weather Forecast Quality in the Alpine Region, *Bull. Amer. Meteor.*, **90**, S28-S32.
- _____, and Co-authors 2009: Supplement to MAP D-PHASE: Real-Time Demonstration of Weather Forecast Quality in the Alpine Region: Additional Applications of the D-Phase Datasets, *Bull. Amer. Meteor.*, **90**, 1321-1336.
- Sills, D. M. L. and P. W. S. King, 1998: The 1997 ELBOW project: High resolution modeling of lake breezes in a pre-storm environment. Preprints, *19th Conf. on Severe Local Storms*, Minneapolis, MN, Amer. Meteor. Soc., 23–26.
- Sills, D. M. L., and N. M. Taylor, 2008: The Research Support Desk (RSD) initiative at Environment Canada: Linking severe weather researchers and forecasters in a real-time operational setting. Preprints, *24th AMS Conference on Severe Local Storms*, Savannah, GA., Amer. Meteorol. Soc., Paper 9A.1.
- Tanguay, M., A. Robert, R. Laprise, 1990: A Semi-implicit Semi-Lagrangian Fully Compressible Regional Forecast Model, *Mon. Wea. Rev.*, **118**, 1970-1980.
- Taylor, N. M., D. M. L. Sills, J. M. Hanesiak, J. A. Milbrandt, C. D. Smith, G. S. Strong, S. H. Skone, P. J. McCarthy, and J. C. Brimelow, 2010: The Understanding Severe Thunderstorms and Alberta Boundary Layers Experiment (UNSTABLE) 2008. Submitted to *Bull. Amer. Meteor.*.
- Taylor, N., D. Sills, J. Hanesiak, J. Milbrandt, P. McCarthy, C. Smith and G. Strong, 2007: The UNderstanding Severe Thunderstorms and Alberta Boundary Layers Experiment (UNSTABLE): a report following the first science workshop, 18-19 April 2007, Edmonton, Alberta, *CMOS Bulletin SCMO*, **35**, 20-28.
- Taylor, N. M., D. M. L. Sills, J. Hanesiak, J. A. Milbrandt, C. D. Smith, G. Strong, S. Skone, P. J. McCarthy, and J. Brimelow, 2008: The Understanding Severe Thunderstorms and Alberta Boundary Layers Experiment (UNSTABLE): Overview and preliminary results. Preprints, *24th AMS Conference on Severe Local Storms*, Savannah, GA, Amer. Meteorol. Soc., Paper 18.7.
- Yeh, K.-S., J. Côté, S. Gravel, A. Méthot, A. Patoine, M. Roch, A. Staniforth, 1998: The Operational CMC–MRB Global Environmental Multiscale (GEM) Model. Part III: Non-hydrostatic Formulation, *Mon. Wea. Rev.*, **130**, 339-356.

